Impact of Synchronization Phase Dynamics on DQ Impedance Measurement

Gong, Hong; Yang, Dongsheng; Wang, Xiongfei

Published in:
2018 IEEE 19th Workshop on Control and Modeling for Power Electronics, COMPEL 2018

DOI (link to publication from Publisher):
10.1109/COMPEL.2018.8458487

Publication date:
2018

Document Version
Accepted author manuscript, peer reviewed version

Impact of Synchronization Phase Dynamics on DQ Impedance Measurement

Hong Gong, Dongsheng Yang, Xiongfei Wang
Department of Energy Technology
Aalborg University
Aalborg, Denmark
hgo@et.aau.dk, doy@et.aau.dk, xwa@et.aau.dk

***Abstract*—Small-signal stability assessment of the three-phase system can be performed using the measured impedances of the load and source. To obtain the dc steady-state operation point, the impedances are measured in the rotating *dq*-frame, and the phase angle is needed for the coordinate transformation used in both the perturbation injection and the impedance calculation. However, the phase estimation may introduce additional dynamics, affecting the accuracy of impedance measurement. This paper investigates the impact of phase synchronization dynamics on the measured impedance results. It is revealed that the phase variations in the perturbation injection has little effect on the measured impedance, while the phase dynamics introduced in the impedance calculation may have a significant impact. Based on impedance transformation, a new impedance calculation method is proposed, which can reduce the errors caused by the phase dynamics. Finally, the simulation and experiment results verify the accuracy of the analytical results and the effectiveness of the proposed method.**

Keywords—Small-signal model, synchronization phase, impedance measurement, dq-frame, impedance transformation

I. INTRODUCTION

The impedance-based stability analysis method has been widely applied in the power-electronics-based power system [1], [2]. In the case of three-phase system, the small-signal impedance model can be developed in the rotating *dq*-frame for stability analysis [3]. However, the analytical *dq* impedance model is difficult to be obtained because system operators have no access to the detailed data of power converters. Thus, there is a huge demand for impedance measurement in the *dq*-frame.

In practical system, there are no d-axis or q-axis terminals for voltage and current measurements. The voltage and current have to be measured in the abc-frame via sensors first and then transformed into *dq*-frame. Similarly, the perturbation is usually designed in the *dq*-frame and then transformed into the abc-frame. Hence, in order to measure the impedance model in the *dq*-frame, the synchronization phase has to be estimated for the coordinate transformation. In general, the phase can be obtained by using PLL or other algorithms. However, among many *dq*-impedance measurement methods, few of them have considered the impact of the phase dynamics on the impedance measurement. A three-phase bridge converter or wound rotor induction machine operating at the synchronous speed are used to inject the current perturbation in [4]. This work does not explain how to obtain the synchronization phase angle or how the synchronization phase angle affects the impedance measurement results. Using Fast Fourier Transform (FFT) on the grid voltage, the phase information can be calculated directly [5]. However, a small frequency drift of the grid voltage during the impedance measurement will result in large phase errors. To overcome this drawback, PLL for the grid synchronization of the current control is directly used to provide the synchronization phase for the perturbation injection and impedance calculation [6], [7]. Since the control bandwidth of this PLL is relatively high, it may lead to large errors, especially in the low-frequency range [8]. In order to avoid the error introduced by the synchronization phase angle using PLL, a decoupled perturbation injection method was proposed in [9]. This estimation method only uses the *d*-axis voltage that is not affected by the dynamic influence of the PLL to calculate the grid impedance, which may not be suitable for the measurement of the converter impedance. As for the converter impedance measurement, the bandwidth of the PLL for impedance calculation was usually set much lower than the lowest injected perturbation frequency to reduce these errors cased by the synchronization phase dynamics [10]-[11]. In this case, however, the control bandwidth of the PLL for the impedance calculation has to set extremely low when the injected perturbation frequency is small, e.g. a few Hz, and the low-bandwidth PLL would take a long time to obtain the grid frequency and cannot track the system frequency variations accurately, which significantly influences the impedance measurement results. The influence of PLL dynamics on the accuracy of the impedance measurement results was analyzed and a correction method of the impedance measurement was proposed in [8]. However, the impedance error introduced by PLL cannot be eliminated at the frequency below the bandwidth of the PLL used for impedance calculation.

In order to define the appropriate phase for impedance measurement, this paper analyzes the influence of coordinate transformation angels on the accuracy of the impedance measurement and proposes a new impedance calculation method based on impedance transformation, so as to further reduce the errors caused by the phase dynamics. The effectiveness of the proposed method has been validated by the simulation and experiment results.

II. IMPEDANCE MEASUREMENT IN THE D-Q FRAME

For the balanced and symmetrical three-phase AC system, the *dq* impedance model is widely used, since there exists a dc operation point in the *dq*-frame. Similarly to DC systems, the relationship between small variations of *dq*-axis voltages and currents can be applied to describe the *dq* impedance characteristic of converters. Thus, the small-signal *dq* impedance model of converters can be derived by linearizing voltages and currents around its steady-state operating point, as shown in (1).

$$\begin{bmatrix}\Delta U_d\\ \Delta U_q\end{bmatrix}=\mathbf{Z_{dq}}\begin{bmatrix}\Delta I_d\\ \Delta I_q\end{bmatrix}=\begin{bmatrix}Z_{dd} & Z_{dq}\\ Z_{qd} & Z_{qq}\end{bmatrix}\begin{bmatrix}\Delta I_d\\ \Delta I_q\end{bmatrix} \quad (1)$$

where △ denotes a small-signal variation of the respective variables from the equilibrium point.

However, since in the small-signal analysis the converter acts as a current source, the impedance is presented as an admittance, which can be rewritten as (2)

$$\begin{bmatrix}\Delta I_d\\ \Delta I_q\end{bmatrix}=\mathbf{Y}_{dq}\begin{bmatrix}\Delta U_d\\ \Delta U_q\end{bmatrix}=\begin{bmatrix}Y_{dd} & Y_{dq}\\ Y_{qd} & Y_{qq}\end{bmatrix}\begin{bmatrix}\Delta U_d\\ \Delta U_q\end{bmatrix} \quad (2)$$

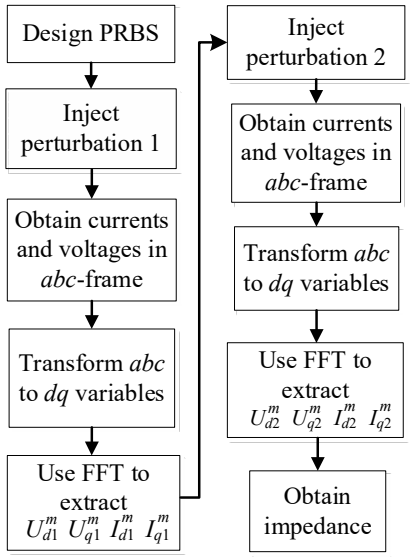

Fig. 1: Impedance measurement procedure.

In general, the basic principle of the impedance measurement is to inject the perturbation into the system and then calculate the impedance based on the response of the voltage and current at its terminal. The detailed flowchart of the impedance measurement procedure is shown in Fig.1. As can be seen, in order to obtain the impedance over a wide frequency range and save measuring time, a broadband signal, pseudo random binary sequence (PRBS) is chosen as the excitation signals (perturbations). The magnitude and frequency of this excitation signal must be designed carefully to fully excite the dynamic characteristic of the converter [13]. In general, since the impedance model to be measured is the small-signal impedance model, the magnitude of the PRBS should not exceed 10% of the rated values.

After designing the PRBS signals, the perturbations have to be injected into the system to generate the voltage and current response of the converter. In general, there are two types of perturbation injection methods: shunt current injection that is better for low impedance measurement and series voltage injection that is more suitable for high impedance measurement. In this paper, the shunt current injection is adopted for the impedance measurement of the converter because this method is much easier to implement for the experimental verification. Nevertheless, the type of the injection method does not influence the analysis results of the synchronization phase angle on the impedance measurement.

In order to acquire the specific components of the impedance matrix as shown in (2), two linearly independent perturbations are required to gain enough information. The synchronization phase angle for definition of the perturbation *dq*-frame must be obtained first to guarantee the perturbation to be injected in the corresponding measured *dq*-frame. Based on the synchronization phase angle for the perturbation injection, the PRBS excitation signal with the frequency of interest is firstly generated on the *d*-axis while the *q*-axis perturbation is equal to zero. Similarly, a second PRBS perturbation sequence is implemented but injecting the *q*-axis perturbation instead, with the *d*-axis components being zero.

The measured output current and voltage of the converter are then transformed to the rotating *dq*-frame based on the synchronization phase angle for the impedance calculation. Applying FFT to transformed variables, the magnitude and phase information for each voltage and current at the injected frequency would be extracted at a time.

Based on the extracted magnitude and phase information, the impedance calculation algorithm developed in [10] was used to calculate the converter impedance in the *dq*-frame, which can be calculated as (2).

$$\begin{bmatrix}Y_{dd} & Y_{dq}\\ Y_{qd} & Y_{qq}\end{bmatrix}=\begin{bmatrix}I_{d1}^m & I_{d2}^m\\ I_{q1}^m & I_{q2}^m\end{bmatrix}\begin{bmatrix}U_{d1}^m & U_{d2}^m\\ U_{q1}^m & U_{q2}^m\end{bmatrix}^{-1} \quad (3)$$

where subscript '1, 2' mean two linearly independent perturbations.

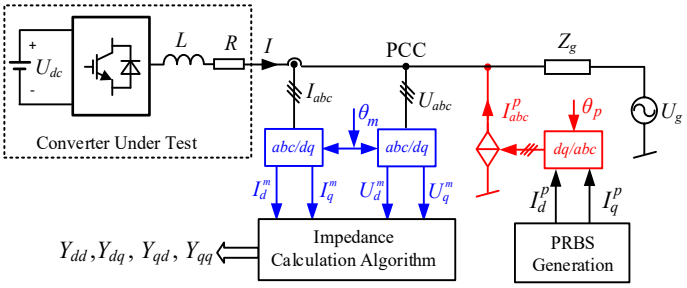

Fig. 2: System diagram of the impedance measurement setup.

Fig. 2 shows the system diagram of the impedance measurement setup. In order to distinguish the influences of synchronization phase angles, two different synchronization phases θ_p and θ_m are used to denote the synchronization phase angles for the perturbation injection and the impedance calculation, respectively. Either PLL or other alternative algorithms can be used to obtain the synchronization phase angles [14]. In this setup, the PLL is adopted to generate the synchronization phase angle for the perturbation injection and impedance calculation. It should be noted that the PLL used for the perturbation injection and the PLL for impedance calculation have nothing to do with the PLL used inside the converter under test. In general, the PCC voltage is considered as the input of PLLs used for both the perturbation injection and impedance calculation so the injected perturbations will definitely influence the output synchronization phase angle of the PLL. The influence of the synchronization phase angle are separated by two parts in respect to the purposes, i.e. the perturbation injection and the impedance calculation, which will be discussed in Section III.

III. Influence of Synchronization Phase Dynamics in Impedance Calculation and Perturbation Injection

A. Influence of Synchronization Phase Dynamics on Perturbation Injection

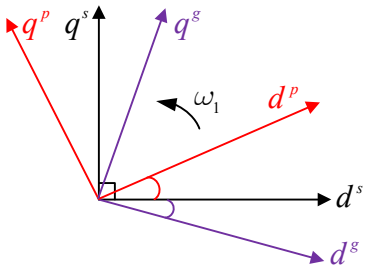

Fig.3: Grid, perturbation and PCC *dq*-frame.

Fig.3 shows the *dq*-frames of the grid-, perturbation- and PCC-voltage. Assuming that the synchronization phase angle for the impedance calculation can be obtained accurately, it is aligned with the PCC *dq*-frame. $\triangle\theta_1+\theta_1$ denotes the angle difference between the perturbation *dq*-frame (θ_p) and PCC *dq*-frame (θ_s), in which $\triangle\theta_1$ is caused by the PLL used for the coordinate transformation of the injected perturbation and θ_1 is the initial phase of the perturbation *dq*-frame. The value of θ_1 determines the proportion of the *d*-axis and *q*-axis perturbation components injected into the system. The relationship between the voltage perturbation $U^p_{pd,q}$ in the perturbation *dq*-frame and in the PCC *dq*-frame is derived as

$$\begin{bmatrix} U^s_{pd0}+U^s_{pd} \\ U^s_{pq0}+U^s_{pq} \end{bmatrix} = \begin{bmatrix} \cos(\theta_1+\Delta\theta_1) & \sin(\theta_1+\Delta\theta_1) \\ -\sin(\theta_1+\Delta\theta_1) & \cos(\theta_1+\Delta\theta_1) \end{bmatrix} \begin{bmatrix} U^p_{pd0}+U^p_{pd} \\ U^p_{pq0}+U^p_{pq} \end{bmatrix} \tag{4}$$

where $U^p_{pd0,q0}$ represents the steady-state value of the perturbation in the perturbation *dq*-frame.

Since $\triangle\theta_1$ is very small, trigonometric functions can be approximate as $\sin\triangle\theta_1\approx\triangle\theta_1$, $\cos\triangle\theta_1\approx1$. By eliminating the steady-state values, (4) can be further derived as

$$\begin{bmatrix} U^s_{pd} \\ U^s_{pq} \end{bmatrix} = \begin{bmatrix} \cos\theta_1 & \sin\theta_1 \\ -\sin\theta_1 & \cos\theta_1 \end{bmatrix} \begin{bmatrix} U^p_{pd} \\ U^p_{pq} \end{bmatrix} - \Delta\theta_1 \begin{bmatrix} \sin\theta_1 & -\cos\theta_1 \\ \cos\theta_1 & \sin\theta_1 \end{bmatrix} \begin{bmatrix} U^p_{pd0} \\ U^p_{pq0} \end{bmatrix} \tag{5}$$

Since the steady-state value of the injected perturbations $U^p_{pd0,q0}$ in the perturbation *dq*-frame are zero, the dynamic influence of the PLL is avoided, as shown in (5). Therefore, the different bandwidth of the PLL for perturbation injection will not influence the accuracy of impedance measurement results.

On the other hand, the relationship between the current perturbation in the perturbation *dq*-frame and in the PCC *dq*-frame can be derived

$$\begin{bmatrix} I^s_{pd} \\ I^s_{pq} \end{bmatrix} = \begin{bmatrix} \cos\theta_1 & \sin\theta_1 \\ -\sin\theta_1 & \cos\theta_1 \end{bmatrix} \begin{bmatrix} I^p_{pd} \\ I^p_{pq} \end{bmatrix} \tag{6}$$

In addition, (5) can be simplified as

$$\begin{bmatrix} U^s_{pd} \\ U^s_{pq} \end{bmatrix} = \begin{bmatrix} \cos\theta_1 & \sin\theta_1 \\ -\sin\theta_1 & \cos\theta_1 \end{bmatrix} \begin{bmatrix} U^p_{pd} \\ U^p_{pq} \end{bmatrix} \tag{7}$$

where different values of θ_1 represent different compositions of the current and voltage perturbations for the calculation of the impedance. In the physical sense, it merely means that the perturbations injected at different electrical point of the system. Base on the current and voltage expression of (6) and (7), the measured admittance expressions $\mathbf{Y}^{\boldsymbol{m}}_{\boldsymbol{dq}}$ can be rewritten as

$$\mathbf{Y}^{\boldsymbol{m}}_{\boldsymbol{dq}} = \begin{bmatrix} \cos\theta_1 & \sin\theta_1 \\ -\sin\theta_1 & \cos\theta_1 \end{bmatrix} \mathbf{Y}^{\boldsymbol{p}}_{\boldsymbol{dq}} \begin{bmatrix} \cos\theta_1 & \sin\theta_1 \\ -\sin\theta_1 & \cos\theta_1 \end{bmatrix}^{-1} = \mathbf{Y}^{\mathbf{s}}_{\boldsymbol{dq}} \tag{8}$$

where $\mathbf{Y}^{\boldsymbol{s}}_{\boldsymbol{dq}}$ represents the admittance matrix of the converter in the PCC *dq*-frame (desired admittance measurement). As can be found from (8), the initial phase for the perturbation injection has no influence on the impedance measurement, which means that where to inject perturbations into the system does not influence the impedance measurement results.

B. Influence of Synchronization Phase Dynamics on Impedance Calculation

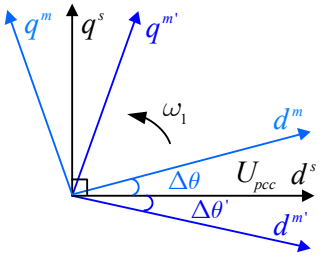

Fig.4 PCC and measured *dq*-frame

After injecting the perturbation into the system, the *abc*-frame voltage and current at converter's terminal are obtained, which are transformed into *dq* quantities based on the synchronization phase angle used for the impedance calculation. If the synchronization phase angle is generated by a PLL, the dynamic impact of the PLL will be superposed on the measured currents and voltages. Assuming the real phase of the PCC voltage is θ and the estimated phase is θ_m, there exists an angle difference between θ and θ_m due to the dynamic influence of the PLL. From the perspective of the measurement, two angle differences, $\triangle\theta$ and $\triangle\theta'$ are caused by the PLL due to two linearly independent perturbations, as shown in Fig.4. Therefore, the relationship between the measured voltages in the PCC *dq*-frame (superscript '*s*') and in the estimated *dq*-frame (superscript '*m*') can be obtained.

$$\begin{bmatrix} U^m_{pd1} \\ U^m_{pq1} \end{bmatrix} = \begin{bmatrix} \cos(\Delta\theta) & \sin(\Delta\theta) \\ -\sin(\Delta\theta) & \cos(\Delta\theta) \end{bmatrix} \begin{bmatrix} U^s_{pd1} \\ U^s_{pq1} \end{bmatrix} \tag{9}$$

$$\begin{bmatrix} U^m_{pd2} \\ U^m_{pq2} \end{bmatrix} = \begin{bmatrix} \cos(\Delta\theta') & \sin(\Delta\theta') \\ -\sin(\Delta\theta') & \cos(\Delta\theta') \end{bmatrix} \begin{bmatrix} U^s_{pd2} \\ U^s_{pq2} \end{bmatrix} \tag{10}$$

Base on formulation (5) and (6), (9) and (10) can be combined as

$$\begin{bmatrix} U^m_{pd1} & U^m_{pd2} \\ U^m_{pq1} & U^m_{pq2} \end{bmatrix} = \begin{bmatrix} 1 & U^s_{q0}G_{PLL} \\ 0 & 1-U^s_{d0}G_{PLL} \end{bmatrix} \begin{bmatrix} U^s_{pd1} & U^s_{pd2} \\ U^s_{pq1} & U^s_{pq2} \end{bmatrix} \quad (11)$$

where U^s_{q0} denotes the q-axis steady-state value of the PCC voltage in the PCC dq-frame.

Similarly, the relationship between the current in the PCC dq-frame and in the estimated dq-frame can be derived as

$$\begin{bmatrix} I^m_{pd1} & I^m_{pd2} \\ I^m_{pq1} & I^m_{pq2} \end{bmatrix} = \begin{bmatrix} I^s_{pd1} & I^s_{pd2} \\ I^s_{pq1} & I^s_{pq2} \end{bmatrix} + \begin{bmatrix} 0 & I^s_{q0}G_{PLL} \\ 0 & -I^s_{d0}G_{PLL} \end{bmatrix} \begin{bmatrix} U^s_{pd1} & U^s_{pd2} \\ U^s_{pq1} & U^s_{pq2} \end{bmatrix} \quad (12)$$

where $I^s_{d0,q0}$ denote the d-axis and q-axis steady-state value of the current in the PCC dq-frame, respectively.

According to (11) and (12), the relationship between the measured admittance $\mathbf{Y}^m_{dq}$ and the real admittance $\mathbf{Y}^s_{dq}$ is derived as

$$\mathbf{Y}^m_{dq} = \left(\mathbf{Y}^s_{dq} + \begin{bmatrix} 0 & I^s_{q0}G_{PLL} \\ 0 & -I^s_{d0}G_{PLL} \end{bmatrix} \right) \cdot \begin{bmatrix} 1 & U^s_{q0}G_{PLL} \\ 0 & 1-U^s_{d0}G_{PLL} \end{bmatrix}^{-1} \quad (13)$$

where a mismatch between the real admittance and measured admittance caused by the dynamic influence of the PLL can be clearly observed. Hence, in order to mitigate this effect on the admittance measurement results, the terms $U^s_{d0}G_{PLL}$ and $I^s_{d0}G_{PLL}$ must be small at the frequency of the interest so that they can be neglected, while the terms $U^s_{q0}G_{PLL}$ and $I^s_{q0}G_{PLL}$ are equal to zero since in this case $I^s_{q0}=0, U^s_{q0}=0$.

IV. Impedance Calculation based on Impedance Transformation

The reason why the measured impedance exists difference is that measured results contain the dynamic influence of the PLL used for the detection of the phase. As can be seen from Fig. 4, the impedance is intended to be measured in the PCC voltage dq-frame. However, the PLL used for tracking the PCC voltage phase brings about phase error $\triangle\theta$ in the impedance measurement, which significantly influence the accuracy of the measurement results. Therefore, based on the impedance transformation, which also has been discussed in [15], the impedance is measured first in the grid dq-frame and then transformed into the PCC voltage dq-frame based on its constant angle difference θ_2, as shown in Fig. 3.

Although there exist perturbations injected into the system, they do not influence the PCC voltage phase, since the perturbations do not contain the fundamental frequency component. In addition, since the grid voltage is constant, the introduction of the PLL does not bring dynamic influence in the impedance measurement. Nevertheless, in the real power system, the gird voltage is difficult to obtain, so this method can only be applied for measuring the impedance of the converter for manufacturers. The relationship between the voltage and current in the PCC- and grid-voltage dq-frames are derived

$$\begin{bmatrix} U^s_d \\ U^s_q \end{bmatrix} = \begin{bmatrix} cos\theta_2 & sin\theta_2 \\ -sin\theta_2 & cos\theta_2 \end{bmatrix} \begin{bmatrix} U^g_d \\ U^g_q \end{bmatrix} \quad (14)$$

$$\begin{bmatrix} I^s_d \\ I^s_q \end{bmatrix} = \begin{bmatrix} cos\theta_2 & sin\theta_2 \\ -sin\theta_2 & cos\theta_2 \end{bmatrix} \begin{bmatrix} I^g_d \\ I^g_q \end{bmatrix} \quad (15)$$

Furthermore, the admittance can be obtained by

$$\mathbf{Y}^s_{dq} = \begin{bmatrix} cos\theta_2 & sin\theta_2 \\ -sin\theta_2 & cos\theta_2 \end{bmatrix} \mathbf{Y}^g_{dq} \begin{bmatrix} cos\theta_2 & -sin\theta_2 \\ sin\theta_2 & cos\theta_2 \end{bmatrix} \quad (16)$$

V. Simulation Validation

In order to verify the theoretical analysis, an impedance measurement setup shown in Fig. 1 is simulated. The measurement frequency is from 1.9Hz to 1000Hz and its magnitude is chosen as 10% of the rated current. Table I shows the parameters of the converter under test. Since the admittance of Y_{dd} and Y_{qq} are much larger than the admittance of Y_{dq} and Y_{qd} [16], only the measured results of Y_{dd} and Y_{qq} are provided in this paper for simplicity.

TABLE I. Parameters of the Converter Under Test

Symbol	Description	Value
K_{i_p}/K_{i_i}	Current inner controller	6/1000
K_p/K_i	PI controller of PLL	0.47/44.4
ω	Grid frequency	314 rad/s
f_s	Sampling frequency	10 *k*Hz
I_{d0}	*d* channel current steady value	8 A
I_{q0}	*q* channel current steady value	0 A
U_{d0}	*d* channel voltage steady value	400 V
U_{q0}	*q* channel voltage steady value	0 V
U_{dc0}	DC voltage of converter	730 V
U_g	Grid phase-phase peak voltage	400 V
L	Filtered inductor	1.5 mH
C_g	Grid capacitor	15 μF
L_g	Grid inductor	7.5 mH

TABLE II. Controller Parameters for Different Cases

Case	PLL K_{PLL_p}/K_{PLL_i}	Bandwidth	Initial Phase
Case 1	0.01/0.04	0.4 Hz	0°
Case 2	0.47/44.4	28.2Hz	90°
Case 3	0.01/0.04	0.4Hz	0°
Case 4	0.03/0.20	2.0 Hz	0°
Case 5	0.47/44.4	28.2 Hz	0°

In order to investigate the influence of the synchronization phase angle on the impedance measurement results, five cases are designed, as shown in Table II. Case 1 and Case 2 have different initial phase and bandwidths of PLL for perturbation injection, while Cases 3-5 have different bandwidths of PLL for impedance calculation.

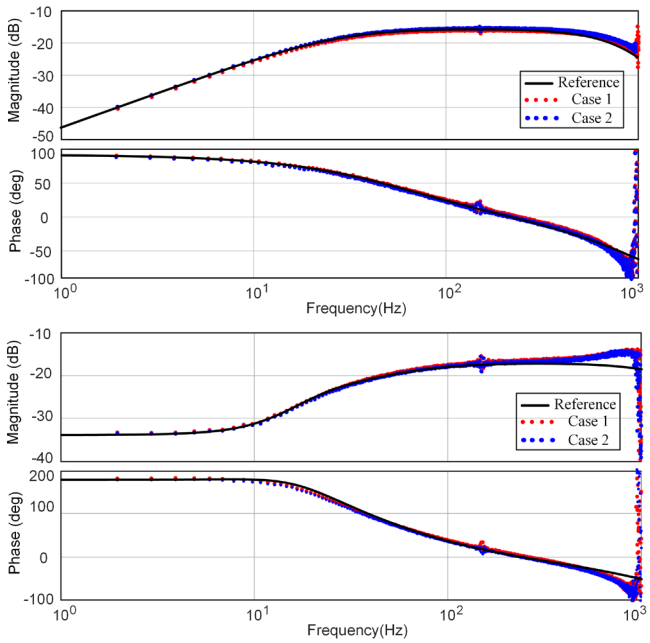

Fig.5: The admittance of Y_{dd} (top) and Y_{qq} (below) under different angle for perturbation injection.

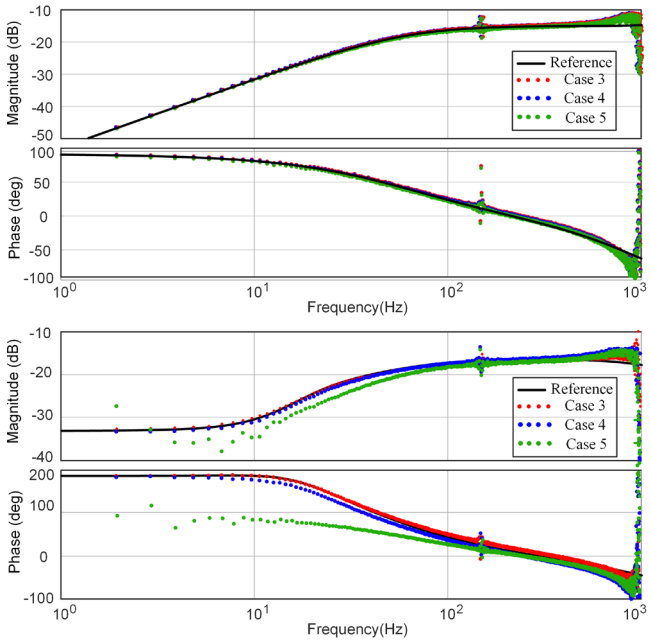

Fig.6: The admittance of Y_{dd} (top) and Y_{qq} (below) under different bandwidth of PLL for impedance calculation.

Fig.5 shows the admittance of Y_{dd} and Y_{qq} under different angles used for the perturbation injection. It is clear that the synchronization angle for perturbation injection has little influence on the impedance measurement. This is mainly because that the perturbation is only used for exciting the response of the system and does not influence the impedance measurement results.

Fig. 6 shows the admittance of Y_{dd} and Y_{qq} under different bandwidth of PLL used for impedance calculation. The bandwidth of Case 3 (0.4Hz) and Case 5 (28.2Hz) are much lower and higher than the lowest perturbation frequency (1.9Hz), respectively, while the bandwidth of Case 4 is close to 1.9Hz. As can be seen, the bandwidth of PLL does not influence the measurement results of Y_{dd}, On the other hand, the bandwidth of PLL significantly influence the measured admittance of Y_{qq}. The higher the bandwidth of PLL is, the larger the measured error is.

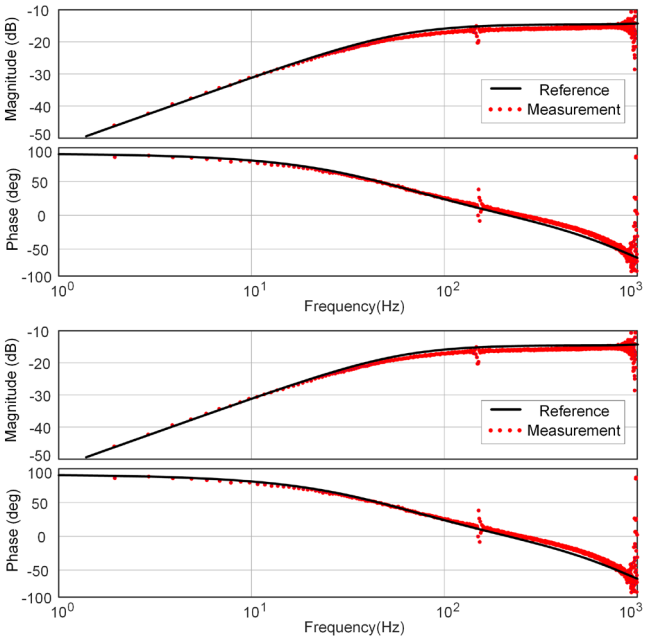

Fig.7: The admittance of Y_{dd} (top) and Y_{qq} (below) based on impedance transformation.

Fig.7 shows the comparison between the theoretically calculated admittance of converter and the measured admittance based on the impedance transformation. The compared results show that the proposed impedance measurement method can obtain the admittance of inverter accurately and is not affected by PLL.

VI. EXPERIMENT VALIDATIONS

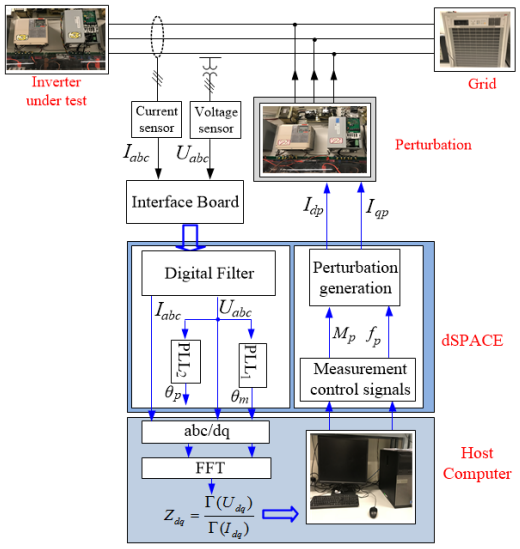

Fig.8: Small-scale prototype of the impedance measurement.

In order to further verify the effectiveness of the analysis results and the proposed method, a small-scale prototype

based on the proposed impedance measurements setup is built.

Fig. 8 shows the detailed experimental setup of the impedance measurement unit. A programmable three-phase voltage source is used to emulate the power grid. Two Danfoss converters were used, one was considered as the inverter under test, the other is used as the source of the perturbation injection. The *dq*-domain output admittance of the inverter was measured to validate the theoretical analysis on the impact of the sysnchronization phase angle used for impedance measurement. The current transducer LA 55-P and voltae transducer LV 25-P are used to acquire current and voltage signals for the calculation of the impedance. The sampled voltage and current were sent to the dSPACE and the synchronization phase was calculated based on the PLL and the voltage and current were recorded in the *dq*-domain.

In addition, the data are processed in the host computer and the impedance are calculated based on the impedance measurement algorithm. It is noted that all the measured admittance resluts appear spike around 50Hz in the *dq*-frame. This is due to the existed background harmonic and does not influence the analysis results on the influence of the synchronization phase angle on the perturbation injection and the impedance calculation.

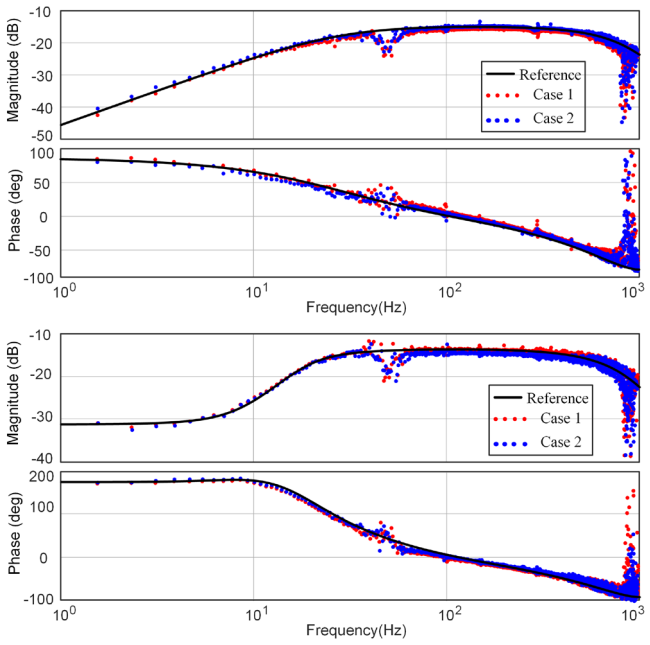

Fig.9: Admittance of Y_{dd} (top) and Y_{qq} (below) under different synchronization angle for perturbation injection.

Fig. 9 shows the admittance of Y_{dd} and Y_{qq} under different synchronization angles used for the perturbation injection. Comparing with Fig.5, the bandwidth of the PLL and the initial phase angle for the perturbation injection would not influence the impedance measurement results, which match with the simulation results. Fig.10 shows the admittances of Y_{dd} and Y_{qq} under the different synchronization angles for the impedance calculation. Both the experiment and simulation results draw the same conclusion that the lower bandwidth of the PLL is preferred to obtain accurate measurement results. Fig. 11 shows the measured admittance results of Y_{dd} and Y_{qq} based on the proposed method. When the estimation method of synchronization phase proposed in this paper is adopted, the influence of the injected perturbations on the impedance measurement results would be mitigated.

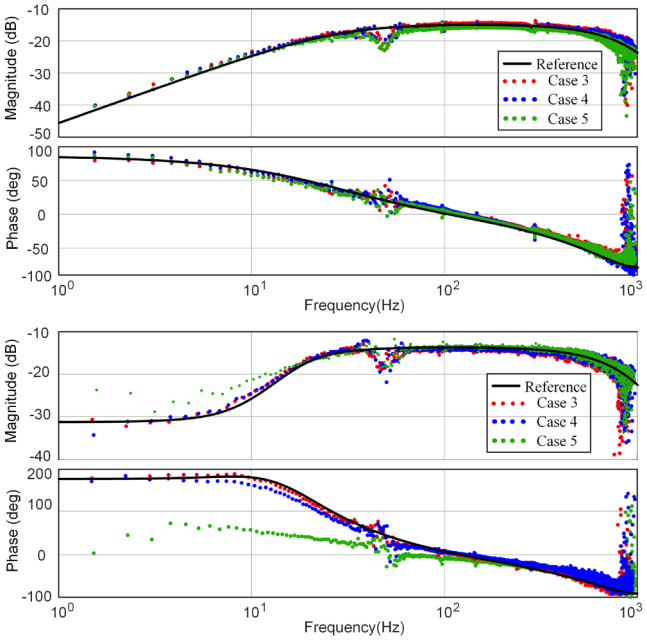

Fig.10: Admittance of Y_{dd} (top) and Y_{qq} (below) under different bandwidth of PLL for impedance calculation.

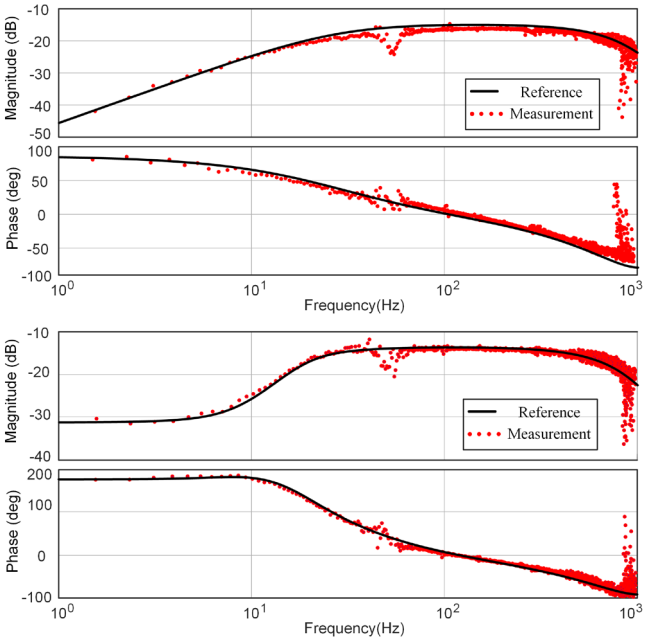

Fig.11: Admittance of Y_{dd} (top) and Y_{qq} (below) based on the proposed method.

VII. CONCLUSION

This paper has analyzed the influence of the synchronization phase on the definition of dq-frame used for the impedance measurement. The analysis has shown that the dynamics of the phase angle used for the impedance calculation have significant influences on the measurement results while the dynamics of the phase used for the perturbation injection has little impact on the impedance measurement. Base on the impedance transformation, a new impedance calculation method is proposed which can

mitigate the influence of phase dynamics and obtain the impedance accurately. The accuracy of the theoretical analysis and the effectiveness of the proposed method have been confirmed by the simulation and experiment results.

REFERENCES

[1] X. Wang and F. Blaabjerg, "Harmonic Stability in Power Electronic Based Power Systems: Concept, Modeling, and Analysis," *IEEE Trans. Smart Grid*. pp.1-1, Mar. 2018

[2] J. Sun, "Impedance-based stability criterion for grid-connected inverters," *IEEE Trans. Power Electron.,* vol. 26, no. 11, pp. 3075–3078, April. 2011.

[3] W. Cao, Y. Ma, L. Yang, F. Wang and L. M. Tolbert, "D–Q impedance based stability analysis and parameter design of three-phase inverter-based AC power systems," *IEEE Trans. Ind. Electron*., vol. 64, no. 7, pp. 6017-6028, July.2017.

[4] Y. L. Familiant, K. A. Corzine, J. Huang and M. Belkhayat, "AC impedance measurement techniques," in *Proc. IEEE Inter. Conf. Electric Mach. Drive.*, May. 2005, pp. 1850-1857.

[5] J. Huang, "AC/DC power system small-signal impedance measurement for stability analysis," Ph.D dissertation, Dept. Elect. Eng., Missouri University of Science and Technology, Missouri, USA, 2009.

[6] T. Roinila, M. Vilkko, and J. Sun, "Broadband methods for online grid impedance measurement," in *Proc. Energy Convers. Congr. Expo.,* Sep. 2013, pp. 3003–3010.

[7] T. Messo, R. Luhtala, T. Roinila, D. Yang, X. Wang, and F. Blaabjerg, "Real-Time impedance-based stability assessment of grid converter interactions," in *Proc. 18th Workshop on Control and Modeling for Power Electronics (COMPEL)*, June. 2017, pp. 1-8.

[8] Z. Shen, M.Jaksic, B.Zhou, P.Mattavelli, J.Verhulst, M.Belkhayat, "Analysis of Phase Locked Loop (PLL) influence on DQ impedance measurement in three-phase AC systems," in *Proc. Appl. Power Electron. Conf. Expo.,* Mar. 2013, pp. 939–945.

[9] J. H. Cho, K. Y. Choi, Y. W. Kim and R. Y. Kim, "A novel P-Q variations method using a decoupled injection of reference currents for a precise estimation of grid impedance," in *Proc. Energy Convers. Congr. Expo.,* Sep. 2014, pp. 5059-5064.

[10] G. Francis, "An algorithm and system for measuring impedance in DQ coordinates," Ph.D. dissertation, Dept. Elect. Eng., Virginia Tech, Blacksburg, USA, 2010.

[11] R. Luhtala, T. Messo, T. Reinikka, J. Sihvo, T. Roinila and M. Vilkko, "Adaptive control of grid-connected inverters based on real-time measurements of grid impedance: DQ-domain approach," in *Proc. Energy Convers. Congr. Expo., Sep.* 2017, pp. 69-75.

[12] B. Miao, R. Zane and D. Maksimovic, "System identification of power converters with digital control through cross-correlation methods," IEEE *Trans. Power Electron.*, vol. 20, no. 5, pp. 1093-1099, Sep. 2005.

[13] T. Roinila, M. Vilkko and J. Sun, "Online grid impedance measurement using discrete-interval binary sequence injection," in *Proc. 14th Workshop on Control and Modeling for Power Electronics (COMPEL)*, June. 2013, pp. 1-8.

[14] Z. Shen. "Online measurement of three-phase AC power system impedance in synchronous coordinates" Ph.D. dissertation, Dept. Elect. Eng., Virginia Tech, Blacksburg, USA, 2012.

[15] A. Rygg, M. Molinas, E. Unamuno, C. Zhang and X. Cai, "A simple method for shifting local dq impedance models to a global reference frame for stability analysis," available in arXiv, https://arxiv.org/pdf/1706.08313.pdf.

[16] B. Wen, D. Boroyevich, R. Burgos, P. Mattavelli and Z. Shen, "Small-signal stability analysis of three-phase AC systems in the presence of constant power loads based on measured d-q frame impedances", *IEEE Trans. Power Electron.*, vol. 30, no. 10, pp. 5952-5963, Oct. 2015.